A planar chiral nanostructure with asymmetric transmission of linearly polarized wave and huge optical activity in near-infrared band*

Liu Dao-Ya(刘道亚), Luo Xiao-Yang(罗孝阳), Liu Jin-Jing(刘锦景), and Dong Jian-Feng(董建峰)†

Institute of Optical Fiber Communication and Network Technology, Ningbo University, Ningbo 315211, *China*

(Received 13 May 2013; revised manuscript received 2 July 2013)

Just like an electronic diode that allows the electrical current to flow in one direction only, a kind of chiral metamaterial structure with a similar functionality for the electromagnetic wave is proposed. The designed nanostructure that consists of twisted metallic split-ring resonators on both sides of a dielectric substrate achieves asymmetric transmission for a forward and backward propagating linearly polarized wave by numerical simulation in near-infrared band. Difference in transmission efficiency of the optimized structure between the same polarized waves incident from opposite directions can reach a maximum at the communication wavelength (1.55 μm). Moreover, the simulation results of this structure also exhibit strong optical activity and circular dichroism.

Keywords: asymmetric transmission, optical activity, linearly polarized wave, circular dichroism

PACS: 42.25.Bs, 42.25.Ja **DOI:** 10.1088/1674-1056/22/12/124202

1. Introduction

Metamaterials have attracted extensive attention due to their unique electromagnetic properties and applications such as negative refraction phenomenon,[1] perfect lens,[2] invisible cloaks,[3,4] etc. The first negative index metamaterial made by Smith and Kroll,[5] and Smith *et al.*,[6] consists of two sections: one is continuous periodic thin metallic rods which provide negative permittivity[7] and the other is split-ring resonators which provide negative permeability.[8] A number of research groups have paid attention to achieving negative permittivity and permeability in recent years.[9] Another method of realizing negative index is to use the chiral structure proposed by Pendry[10] and Tretyakov,[11,12] independently. So over the next few years, many articles about chiral metamaterials were published.[13–22] In chiral metamaterials, neither ε nor μ needs to be negative. What is more, it is easier to achieve negative refractive index by using the huge optical activity of chiral structure rather than by using the "double negative" method.

In the past few years, planar chiral metamaterial has aroused great interest, owing to its other novel property: asymmetric transmission. Since Fedotov *et al.*[23] first observed asymmetric transmission phenomenon by using lossy anisotropic planar chiral fish-scale in 2006, some sophisticated models have been reported on planar chiral metamaterials to achieve asymmetric transmission in microwave,[24–35] THz,[36] and even optical[37–40] frequency regions. Plum *et al.*[25] demonstrated that the transmission and reflection of circular polarization waves through and from planar split-ring microwave metamaterials depend on the incidence direction. Kang *et al.*[28] reported that linearly polarized wave propagating through a certain chiral slab structure can achieve asymmetric transmission in the microwave range. Singh *et al.*[36] presented that a planar metamaterial, an array of coupled metal split-ring resonators with a unit cell lacking mirror symmetry, exhibited asymmetric transmission of terahertz radiation (0.25 THz–2.5 THz) for circular polarization waves propagating through it in opposite directions. Drezet *et al.*[38] experimentally showed that twisted planar nanostructured metallic spiral wires could achieve asymmetric transmission for circularly polarized waves in the visible domain. However, limited by the manufacturing process and experimental verification, fewer reports about asymmetric transmission in the terahertz or optical regime have come out in the literature. Unlike the conventional Faraday effect, the planar chiral metamaterial could also change the polarized state of the incident wave via the interaction of an electromagnetic wave with it but requires no magnetized media.[23,31] In addition, the conventional magnetic devices are often provided with the bulk volume which are not convenient for integration and miniaturization.

In this paper, we design a planar chiral nanostructure that consists of the twisted metallic split-ring resonators (SRRs) on both sides of a substrate. This structure can not only achieve huge optical activity and circular dichroism but also obtain the asymmetric transmission of a linearly polarized wave by numerical simulation. The designed structure with asymmetric

*Project supported by the National Natural Science Foundation of China (Grant No. 61078060), the Fund from the Ningbo Optoelectronic Materials and Devices Creative Team, China (Grant No. 2009B21007), and partially sponsored by K. C. Wong Magna Fund in Ningbo University.

†Corresponding author. E-mail: dongjianfeng@nbu.edu.cn, nbu-djf@21cn.com

© 2013 Chinese Physical Society and IOP Publishing Ltd

transmission property that exhibits unidirectional transmission of the x- or y-polarized waves in a certain direction is analogous to an electronic diode that conducts current in only one direction. Like the reported three-layer ultrathin chiral structure which can realize the functionality of an electronic diode in the microwave regime,[30] our chiral metamaterial structure can achieve the same function in the near-infrared band. Due to the above properties, it provides some potential applications in photonic devices such as isolators and circulators.

2. Theoretical analysis

Assume that a linearly polarized wave propagates through a certain planar chiral medium. The electric field of the incident wave, on the condition that the direction of the incident wave is along $+z$ direction, can be expressed as

$$\boldsymbol{E}^i(\boldsymbol{r},t) = E_i^x \,\mathrm{e}^{\mathrm{j}(kz-\omega t)}\boldsymbol{e_x} + E_i^y \,\mathrm{e}^{\mathrm{j}(kz-\omega t)}\boldsymbol{e_y}, \tag{1}$$

where k, ω, E_i^x, and E_i^y represent the propagation constant, angular frequency, complex incident electric field intensities of x and y directions, respectively. In the same way we can obtain the transmitted wave as

$$\boldsymbol{E}^t(\boldsymbol{r},t) = E_t^x \,\mathrm{e}^{\mathrm{j}(kz-\omega t)}\boldsymbol{e_x} + E_t^y \,\mathrm{e}^{j(kz-\omega t)}\boldsymbol{e_y}. \tag{2}$$

In order to better understand the above equations, we utilize the so-called Jones matrix to describe the relationships between incident and transmitted electric fields as[41]

$$\begin{pmatrix} E_t^x \\ E_t^y \end{pmatrix} = \begin{pmatrix} t_{xx} & t_{xy} \\ t_{yx} & t_{yy} \end{pmatrix} \begin{pmatrix} E_i^x \\ E_i^y \end{pmatrix}, \tag{3}$$

where the first subscript indicates the polarization (x- or y-polarized) of transmitted wave and the second subscript indicates the polarization of the incident wave. Then, the total transmissions for x and y-polarized incident wave can be calculated as $T_x = |t_{xx}|^2 + |t_{yx}|^2$ and $T_y = |t_{xy}|^2 + |t_{yy}|^2$, respectively.

The relation between linearly and circularly polarized waves, on the assumption that the wave propagates in the $+z$ direction, can be given as

$$\begin{aligned} T_{\mathrm{cir}}^{+} &= \begin{pmatrix} t_{++} & t_{+-} \\ t_{-+} & t_{--} \end{pmatrix} \\ &= \frac{1}{2}\begin{pmatrix} t_{xx}+t_{yy}+\mathrm{i}(t_{xy}-t_{yx}) & t_{xx}-t_{yy}-\mathrm{i}(t_{xy}+t_{yx}) \\ t_{xx}-t_{yy}+\mathrm{i}(t_{xy}+t_{yx}) & t_{xx}+t_{yy}-\mathrm{i}(t_{xy}-t_{yx}) \end{pmatrix}, \end{aligned} \tag{4}$$

where the superscript $+$ refers to $+z$ direction while the subscripts cir, $+$ and $-$ denote circularly polarized state, right-handed circularly polarized (RCP), and left-handed circularly polarized (LCP) waves, respectively.

For the linearly polarized incident wave, the asymmetric transmission parameter[40] for the x polarization is described as

$$\Delta_{\mathrm{lin}}^{(x)} = |t_{yx}|^2 - |t_{xy}|^2 = -\Delta_{\mathrm{lin}}^{(y)}. \tag{5}$$

For the circularly polarized incident wave, the asymmetric transmission parameter can be obtained as

$$\Delta_{\mathrm{cir}}^{(+)} = |t_{-+}|^2 - |t_{+-}|^2 = -\Delta_{\mathrm{cir}}^{(-)}. \tag{6}$$

Owing to the sub-wavelength periodicity (the periodic constant is 500 nm which is about one-third of the communication wavelength of 1550 nm) of our designed structure, the chiral metamaterial does not present diffraction phenomenon and can be viewed as an isotropic medium for the incident wave. The optical activity can be described as the polarization azimuthal rotation angle $\theta = (1/2)\,[\arg(t_{++}) - \arg(t_{--})]$ and circular dichroism $\Lambda = |T_{++}| - |T_{--}|$, respectively.

3. Designed chiral structure and simulation method

The proposed chiral nanostructure is composed of two metallic split-ring resonators on both sides of a dielectric layer which is periodic in x and y directions while the z direction is open for inputting and detecting plane waves. The structure is two-dimensionally chiral because its image in a plane mirror of the unit cell cannot be brought to coincidence with itself unless it is lifted off the plane. We choose metallic silver as the material of our designed SRRs because of its low loss[20] in the near-infrared band. A schematic diagram of the unit cell of this structure with all geometric parameters is depicted in Fig. 1.

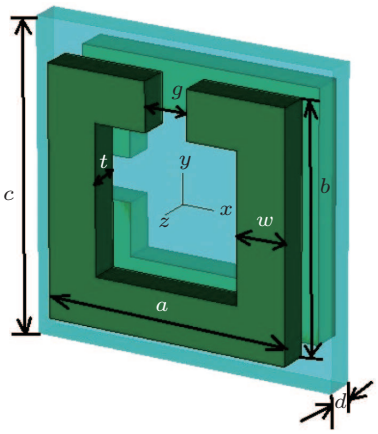


Fig. 1. (color online) Geometry of the chiral unit cell.

The periodic constant c is 500 nm, and the squared substrate is made of silica with a permittivity of 2.1 and thickness $d = 50$ nm. The SRRs on both sides of the substrate are twisted 90 degrees with respect to each other. The parameters of our designed nanostructure are as follows: length $a = b = 400$ nm, top gap $g = 70$ nm, width $w = 80$ nm, and thickness $t = 80$ nm. We do our simulation with finite integration technique,[29] and the unit cell as shown in Fig. 1

is handled with periodic boundary conditions in the simulation. The metallic silver is dealt with the Drude model[20] ($\omega_p = 2\pi \times 2175$ THz, $\omega_c = 2\pi \times 4.35$ THz).

4. Numerical results and discussion

4.1. Asymmetric transmission

To begin with, we use the linearly polarized waves propagating through the planar chiral nanostructure in the x and y directions. The coefficients of linear transmission t_{xx}, t_{xy}, t_{yx}, and t_{yy} are obtained as shown in Fig. 2. Figures 2(a) and 2(b) show the transmission matrix elements of the wave propagation in backward $(-z)$ and forward $(+z)$ directions, respectively. From Fig. 2(a), we can see that there are two resonant peaks for cross-polarization transmission t_{yx}, one reaches 0.9 at a wavelength of 1.69 μm, and the other reaches about 0.93 at the communication wavelength (1.55 μm). However, the other cross-polarization transmission t_{xy} is extremely low across the whole wavelength range in the simulation. At the communication resonant wavelength, the difference between t_{xy} and t_{yx} reaches a maximum of around 0.9. From Figs. 2(a) and 2(b) it follows that the coefficients of the co-polarization transmission t_{xx} and t_{yy} always maintain the same manner no matter which direction the wave propagates in. The significant difference between the two cross-polarization transmissions (t_{xy} and t_{yx}) may contribute to the polarization conversion of the designed structure. When the y-polarized (x-polarized) wave normally propagates through the slab along the $+z$ $(-z)$ direction, the wave is well coupled to the structure and converted mostly into x-polarized (y-polarized) wave while the wave of the opposite direction is hardly coupled to the structure, resulting in lower conversion efficiency.[31] Since the structure is composed of periodic subwavelength unit cells, in order to better understand whether there exists coupling between unit cells, we simulate the structures with different values of periodic constant c. The simulation results (not shown here) show that both the cross-polarization coefficients and the differences between them become smaller as the periodic constant increases. That is to say, there is coupling between unit cells in our designed chiral metamaterial structure.

Figure 3 shows the total transmissions for the y-polarized wave which is along the two opposite directions. As shown by the numerical simulation results, the total transmission of the y-polarized wave which is along the forward ($+z$ direction) can reach 0.87 while the total transmission is lower than 0.03 in the opposite direction around the resonant wavelength (1.55 μm). The designed chiral nanostructure with this interesting effect is similar to an electronic diode that can allow the electric current to flow through it in one direction while blocking the electric current in the opposite direction.

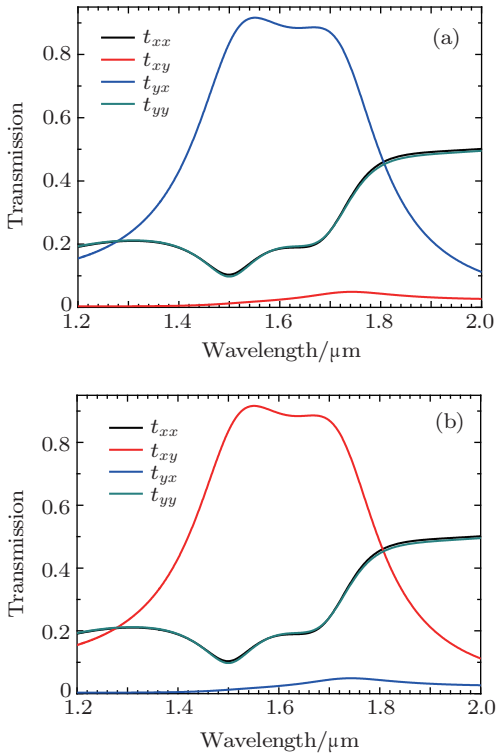


Fig. 2. (color online) The coefficients of backward (a) and forward (b) transmissions.

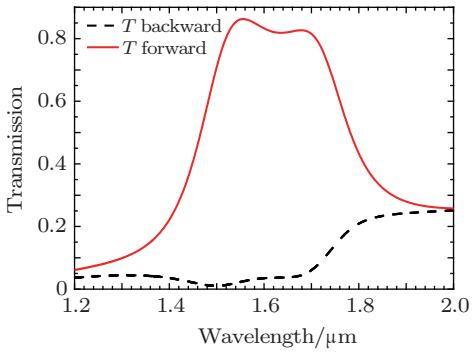


Fig. 3. (color online) The total transmission spectra of y-polarized incident wave propagating through the chiral structure forward (red solid line) and backward (black dashed line).

The calculated values of the asymmetric transmission parameter Δ are shown in Fig. 4. From this graph, we can clearly find that the linearly polarized parameter is in sharp contrast to the circularly polarized wave: the Δ of y-polarized wave which propagates from $+z$ direction can reach about 86% around the resonant wavelength while the parameters of the RCP and LCP are both extremely low across the whole simulation wavelength. Therefore, it is clear that the polarization conversion efficiency of the linearly polarized wave is very high while the circularly polarized wave is low.

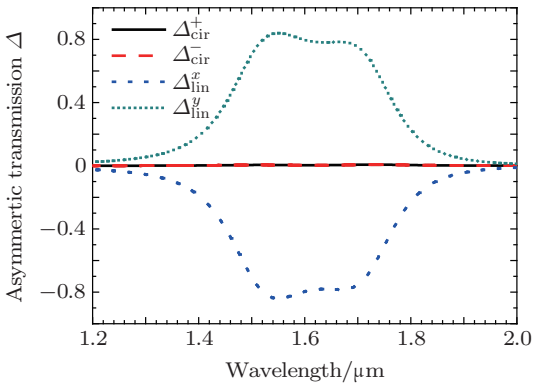


Fig. 4. (color online) Values of asymmetric transmission parameter Δ for linearly and circularly polarized waves along the $+z$ direction.

To look into the transmission efficiency for x or y-polarized wave propagating through the chiral structure forward and backward, we simulate different values of thickness d of substrates and opening sizes (length of the top gap g) of the SRRs. (The reason why we choose the above two parameters is that other variables such as the width of SRRs w, permittivity of the substrate, and the kinds of metal have little effect on the transmission coefficient.) The difference in transmission efficiency of x- or y-polarized incident wave is defined as the asymmetry factor[30] and can be calculated from the following expression:

$$\begin{aligned} \Xi &= \begin{pmatrix} \Xi_x \\ \Xi_y \end{pmatrix} = \begin{pmatrix} T_x^{\rm f} - T_x^{\rm b} \\ T_y^{\rm f} - T_y^{\rm b} \end{pmatrix} \\ &= \begin{pmatrix} (t_{yx}^2 + t_{xx}^2)^{\rm f} - (t_{yx}^2 + t_{xx}^2)^{\rm b}) \\ (t_{xy}^2 + t_{yy}^2)^{\rm f} - (t_{xy}^2 + t_{yy}^2)^{\rm b}) \end{pmatrix}, \end{aligned} \tag{7}$$

where the superscript f indicates forward $(+z)$ direction and b represents backward $(-z)$ direction. Figure 5 illustrates the transmission spectra of y-polarized incident wave for different values of substrate thickness d. From this figure, one can see that as d increases, the transmission efficiency Ξ_y rises, and it can reach a maximum of 0.85 when $d = 50$ nm. However, as the substrate thickness increases, the transmission efficiency descends from the values for the thickness of 50 nm.

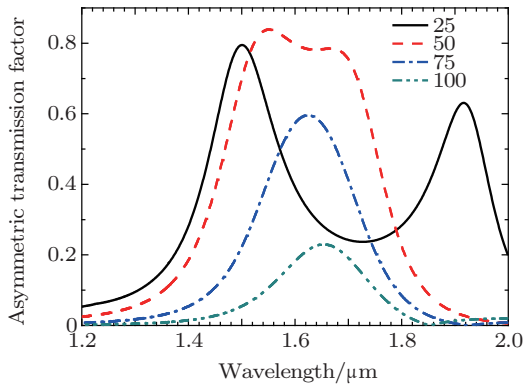


Fig. 5. (color online) Transmission efficiency Ξ_y dependences on substrate thickness for y-polarized incident wave propagating from forward and backward directions.

Since the chiral structure achieves the highest transmission efficiency at the thickness of 50 nm, we chose this thickness to examine the asymmetry factors for different SRR's opening sizes. Figure 6 shows the values of transmission efficiency Ξ_y for the incident linearly polarized wave with respect to the opening sizes of SRR. We can see that each designed model (except for the model of $g = 40$ nm) with $d = 50$ nm exhibits two resonant peaks across the whole simulation wavelength. As the opening size increases, the two resonant peaks move to the left. The bigger the opening size, the lower the resonant wavelength is.

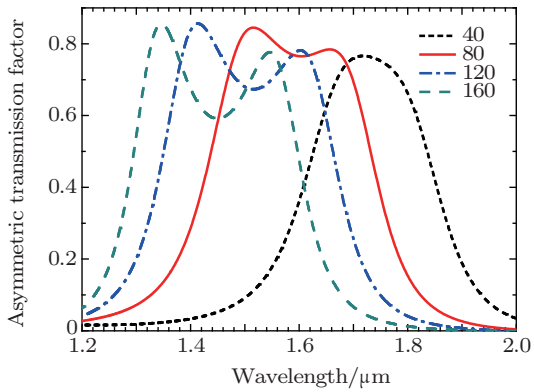


Fig. 6. (color online) Transmission efficiency Ξ_y dependences on the opening size of SRR for y-polarized incident wave propagating from forward and backward directions.

To better understand the mechanism of asymmetric transmission for the linear polarization wave with our designed chiral metamaterial, we analyze the effect of interaction between the nanostructure and x- or y-polarized wave which is travelling through it around the resonant wavelength. Figures 7(a) and 7(b) illustrate the surface electric field distributions for x- and y-polarized wave passing through the designed structure backwards, respectively. It can be clearly seen that the electric field intensity distributed in the gap of the SRR is much stronger for x-polarized wave while there is no intensity distribution in the same gap for y-polarized wave. For the x-polarized wave passing through the nanostructure backwards, the first SRR can be excited efficiently at the resonant wavelength with the wave well coupled into the nanostructure. Then the near-field coupling effect between the first and second SRR results in an obvious y-polarized transmitted wave since the designed structure is two-dimensionally chiral and possesses a huge optical activity (discussed below). However, for the y-polarized wave travelling through the structure along the same direction, it can hardly couple into the chiral metamaterial due to its orientation, not even to mention the near-field coupling effect between the two SRRs. As a consequence, the difference in polarization conversion efficiency between x- and y-polarized waves eventually leads to the asymmetric transmission phenomenon.

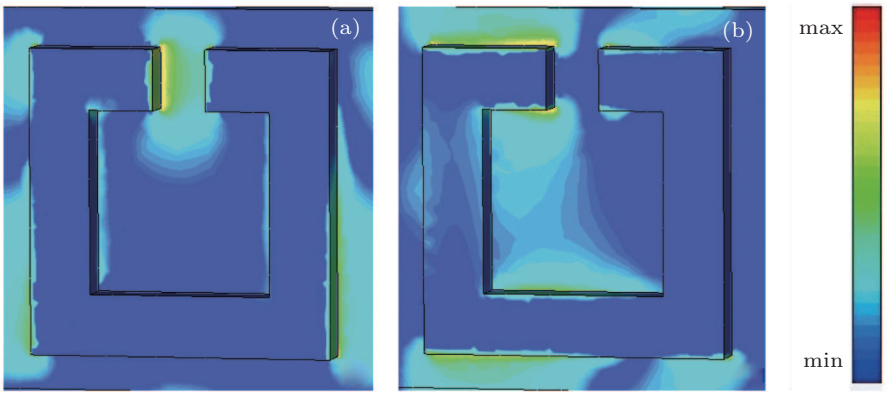


Fig. 7. (color online) Calculated surface electric field distributions for (a) x- and (b) y-polarized waves at the resonant wavelength (1.55 μm).

4.2. Optical activity and circular dichroism

In addition, we also calculate the transmission coefficient spectra of LCP (T_{--}) and RCP (T_{++}) waves, and show the result in Fig. 8. We can find that T_{--} is in sharp contrast to T_{++} around the resonant wavelength: T_{--} reaches the resonant peak while T_{++} obtains its lowest value at 1.73 μm. We can see from Fig. 9(a) that the polarization rotation angle of this nanostructure can reach about 130 degrees around the resonant wavelength (1.4 μm). Figure 9(b) shows that this optical frequency band chiral structure also has a large circular dichroism at the two resonances. So, according to the above simulation results, the designed structure possesses huge optical activity.

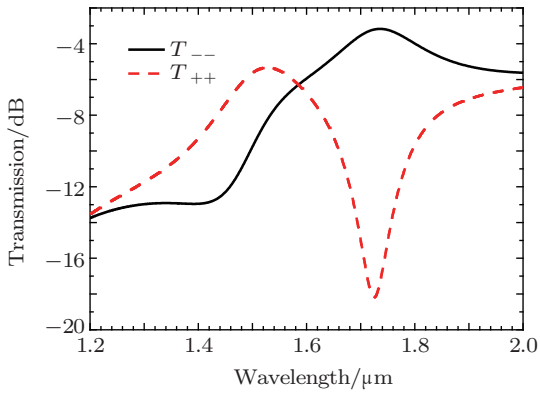


Fig. 8. (color online) Transmission spectra for LCP and RCP waves.

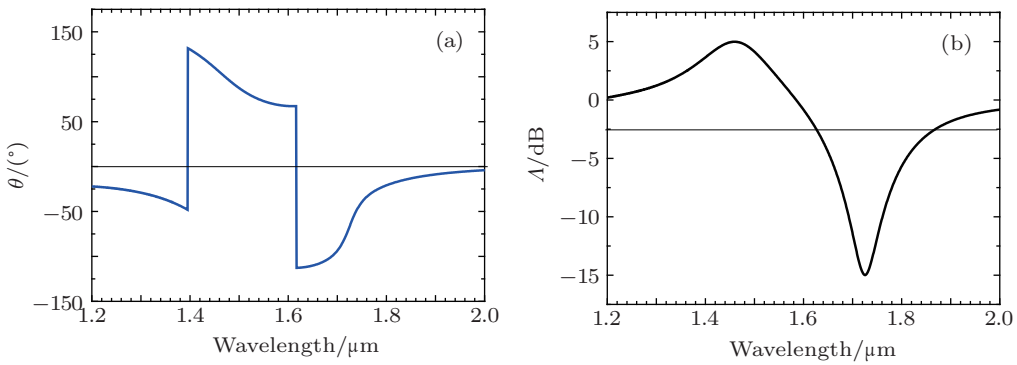


Fig. 9. (color online) (a) Polarization azimuthal rotation angle θ and (b) the circular dichroism Λ.

5. Conclusions

In this paper, the properties of such a chiral metamaterial composed of SRRs on both sides of a substrate are investigated by theoretical analysis and numerical simulation. The results show that the designed structure can achieve asymmetric transmission for the linearly polarized waves in the near-infrared band, which is similar to the function of an electric diode. The difference in polarization conversion efficiency between x- and y-polarized waves results in this novel property. Also, the difference in transmission efficiency of the chiral structure can reach 0.87 at the communication wavelength (1.55 μm) for the x-polarized wave which comes from the $+z$ direction while it is less than 0.03 for the same polarized wave which goes through the opposite direction. We also explore the transmission efficiency dependences on the thickness of substrate and the opening size of SRR, respectively. In addition, the

designed nanostructure can also achieve polarization rotation angle of about 130 degrees at the resonant wavelength. Owing to the asymmetric transmission and huge optical activity and circular dichroism of this designed structure, it provides some potential applications in optical polarization devices such as isolators and circulators.

References

[1] Veselago V G 1968 *Sov. Phys. Usp.* **10** 509
[2] Pendry J B 2000 *Phys. Rev. Lett.* **85** 3966
[3] Schurig D J, Justice B J, Cummer S A, Pendry J B, Starr A F and Smith D R 2006 *Science* **314** 977
[4] Pendry J B, Schurig D J and Smith D R 2006 *Science* **312** 1780
[5] Smith D R and Kroll N 2000 *Phys. Rev. Lett.* **85** 2933
[6] Smith D R, Padilla W J, Vier D C, Nemat-Nasser S C and Schultz S 2000 *Phys. Rev. Lett.* **84** 4184
[7] Pendry J B, Holden A J, Stewart W J and Youngs I 1996 *Phys. Rev. Lett.* **76** 4773
[8] Pendry J B, Holden A J, Robbins D J and Stewart W J 1999 *IEEE. Trans. Microwave Theory Tech.* **47** 2075
[9] Soukoulis C M and Wegener M 2011 *Nat. Photon.* **5** 523
[10] Pendry J B 2004 *Science* **306** 1353
[11] Tretyakov S, Nefedov I, Sihvola A, Maslovski S and Simovski C 2003 *J. Electromagn. Waves Appl.* **17** 695
[12] Tretyakov S, Sihvola A and Jylha L 2005 *Photon. Nanostruct. Fundam. Appl.* **3** 107
[13] Zhou Q L, Shi Y L, Wang A H, Li L and Zhang C L 2012 *Chin. Phys. B* **21** 058701
[14] Xiong H, Hong J S, Jin D L and Zhang Z M 2012 *Chin. Phys. B* **21** 094101
[15] Xiong H, Hong J S and Jin D L 2013 *Chin. Phys. B* **22** 014101
[16] Zhong X Q, Cheng K and Xiang P A 2013 *Chin. Phys. B* **22** 034205
[17] Plum E, Zhou J, Dong J, Fedotov V A, Koschny T, Soukoulis C M and Zheludev N I 2009 *Phys. Rev. B* **79** 035407
[18] Zhang S, Park Y, Li J, Lu X, Zhang W and Zhang X 2009 *Phys. Rev. Lett.* **102** 023901
[19] Zhou J, Dong J, Wang B, Koschny T, Kafesaki M and Soukoulis C M 2009 *Phys. Rev. B* **79** 121104
[20] Dong J, Zhou J, Koschny T and Soukoulis C 2009 *Opt. Express* **17** 14172
[21] Dong J, Li J and Yang F Q 2011 *Prog. Electromagn. Res.* **112** 241
[22] Li J, Yang F Q and Dong J 2011 *Prog. Electromagn. Res.* **116** 395
[23] Fedotov V A, Mladyonov P L, Prosvirnin S L, Rogacheva A V, Chen Y and Zheludev N I 2006 *Phys. Rev. Lett.* **97** 167401
[24] Plum E, Fedotov V A and Zheludev N I 2009 *J. Opt. A: Pure Appl. Opt.* **11** 074009
[25] Plum E, Fedotov V A and Zheludev N I 2009 *Appl. Phys. Lett.* **94** 131901
[26] Plum E, Fedotov V A and Zheludev N I 2011 *J. Opt.* **13** 024006
[27] Han J, Li H and Fan Y 2011 *Appl. Phys. Lett.* **98** 151908
[28] Kang M, Chen J, Cui H X, Li Y and Wang H T 2011 *Opt. Express* **19** 8347
[29] Mutlu M, Akosman A E, Serebryannikov A E and Ozbay E 2011 *Opt. Express* **19** 14290
[30] Mutlu M, Akosman A E, Serebryannikov A E and Ozbay E 2012 *Phys. Rev. Lett.* **108** 213905
[31] Huang C, Feng Y, Zhao J, Wang Z and Jiang T 2012 *Phys. Rev. B* **85** 195131
[32] Huang C, Zhao J, Jiang T and Feng Y 2012 *J. Electromagn. Waves Appl.* **26** 1192
[33] Novitsky A V, Galynsky V M and Zhukovsky S V 2012 *Phys. Rev. B* **86** 075138
[34] Cheng Y, Nie Y, Wang X and Gong R 2013 *Appl. Phys. A* **111** 209
[35] Lin W, Yang Z and Cheng Y Z 2013 *Opt. Express* **21** 5239
[36] Singh R, Plum E and Menzel C 2009 *Phys. Rev. B* **80** 153104
[37] Fedotov V A, Schwanecke A S, Zheludev N I, Khardikov V V and Prosvirnin S L 2007 *Nano Lett.* **7** 1996
[38] Drezet A, Genet C, Laluet J Y and Ebbesen T W 2008 *Opt. Express* **16** 12559
[39] Schwanecke A S, Fedotov V A, Khardikov V V, Prosvirnin S L, Chen Y and Zheludev N I 2008 *Nano Lett.* **8** 2940
[40] Menzel C, Helgert C and Rockstuhl C 2010 *Phys. Rev. Lett.* **104** 253902
[41] Menzel C, Rockstuhl C and Lederer F 2010 *Phys. Rev. A* **82** 053811